RESEARCH ARTICLE

The differential association between local neurotransmitter levels and whole-brain resting-state functional connectivity in two distinct cingulate cortex subregions

Meng Li[1,2,3] | Lena Vera Danyeli[1,3,4] | Lejla Colic[1,2,3] | Gerd Wagner[1,2] | Stefan Smesny[1] | Tara Chand[1,3,4,5] | Xin Di[6] | Bharat B. Biswal[6] | Jörn Kaufmann[7] | Jürgen R. Reichenbach[2,8,9,10] | Oliver Speck[2,11,12,13,14] | Martin Walter[1,2,3,4,5,12] | Zümrüt Duygu Sen[1,2,3,4]

[1]Department of Psychiatry and Psychotherapy, Jena University Hospital, Jena, Germany

[2]Center for Intervention and Research on Adaptive and Maladaptive Brain Circuits Underlying Mental Health, DZP, Germany

[3]Clinical Affective Neuroimaging Laboratory (CANLAB), Magdeburg, Germany

[4]Department of Psychiatry and Psychotherapy, University Tübingen, Tübingen, Germany

[5]Max Planck Institute for Biological Cybernetics, Tübingen, Germany

[6]Department of Biomedical Engineering, New Jersey Institute of Technology, Newark, New Jersey, USA

[7]Department of Neurology, Otto von Guericke University Magdeburg, Magdeburg, Germany

[8]Medical Physics Group, Department of Diagnostic and Interventional Radiology, Jena University Hospital, Jena, Germany

[9]Michael Stifel Center Jena for Data-Driven & Simulation Science (MSCJ), Jena, Germany

[10]Center of Medical Optics and Photonics (CeMOP), Jena, Germany

[11]Department of Biomedical Magnetic Resonance, Otto von Guericke University, Magdeburg, Germany

[12]Center for Behavioral Brain Sciences, Magdeburg, Germany

[13]German Center for Neurodegenerative Diseases (DZNE), Magdeburg, Germany

[14]Leibniz Institute for Neurobiology, Magdeburg, Germany

Correspondence
Zümrüt Duygu Sen and Martin Walter, Department of Psychiatry and Psychotherapy, Jena University Hospital, Philosophenweg 3, 07743 Jena, Germany.
Email: zuemruet.sen@med.uni-jena.de and martin.walter@med.uni-jena.de

Abstract

Reproducible resting-state functional connectivity (rsFC) patterns and their alterations play an increasing role in neuropsychiatric research. Studies that limit the analysis of metabolites and *rsFC strengths* to a predefined canonical network suggest that the *rsFC strength* positively correlates with the local glutamate (Glu) levels and negatively correlates with the gamma-aminobutyric acid (GABA) levels. The contribution of regional neurotransmitter activity to *rsFC strengths* from a given seed to the whole-brain remains unclear. In this study, 121 healthy participants (50 female/71 male) underwent multimodal resting-state functional magnetic resonance imaging (rsfMRI) and magnetic resonance spectroscopy (MRS) at 7 T, allowing for acquisition of multiple, neuroanatomically well-defined MRS voxels in the same session. We examined the association between rsFC and local neurotransmitter levels in the

pregenual anterior cingulate cortex (pgACC) and the anterior mid-cingulate cortex (aMCC) by varying *rsFC strengths* at the whole-brain level. Our results showed that both glutamatergic and GABAergic *edge weights* (defined as the across-participants partial correlation coefficients between the local metabolite levels and the rsFC of the seed region to each target parcel) were positively correlated with the *rsFC strengths* in the pgACC and negatively correlated with the *rsFC strengths* in the aMCC. The region-dependent directionality of associations may indicate that region-specific microscale properties, such as neurotransmitter receptor architecture, modulate the interaction between brain regions at the macroscale level.

1 | INTRODUCTION

The human brain is organized in multiple functional and structural levels that enable its complex functioning and that are dynamically modulated by the neurotransmitter systems. At the microscale level, the gating of ion channels is modulated by the neurotransmitters that subsequently enable membrane potential dynamics and neuronal firing (Burke & Bender, 2019; Meir et al., 1999). The microscale functioning of a particular brain region depends on its cyto- and chemoarchitecture (Amunts & Zilles, 2015). At the macroscale level, the neural firing of thousands of neurons across different brain areas is integrated to form and maintain the evolving brain states and brain organization (Suárez, Markello, Betzel, & Misic, 2020).

A well-known example of reproducible brain organization is the resting-state activity pattern that can be measured via functional connectivity, known as the resting-state functional connectivity (rsFC) (Biswal, Yetkin, Haughton, & Hyde, 1995; Greicius, Krasnow, Reiss, & Menon, 2003). The rsFC describes the similarity between the neuronal activation patterns of investigated regions by assessing the temporal correlation of blood-oxygen-level-dependent (BOLD) fluctuations (Friston, 1994). RsFC are also reproducible across different participants (Damoiseaux et al., 2006; De Luca, Beckmann, De Stefano, Matthews, & Smith, 2006). Altered rsFC patterns have been found in patients with neuropsychiatric diseases compared to healthy participants and have been suggested as potential biomarkers to predict diagnostic status and/or the severity of the disorders (Greicius, 2008). Nevertheless, the interpretability of the rsFC patterns remains challenging due to an incomplete understanding of the underlying neurobiological characteristics of the BOLD signal and consequently the rsFC (Allan et al., 2015; Friston, 2011; Logothetis, 2003; Logothetis & Wandell, 2004; Mueller et al., 2013; Tagliazucchi, Balenzuela, Fraiman, Montoya, & Chialvo, 2011; Tak, Polimeni, Wang, Yan, & Chen, 2015). A better understanding of the mechanisms that form and maintain the brain's rsFC architecture would lay the foundation for future investigations of brain disorders.

The rsFC patterns are likely to be associated with the cyto- and chemoarchitecture of an observed region. For example, higher overall rsFCs were found in the frontal cortical areas with higher excitatory receptor levels compared to inhibitory receptor levels (van den Heuvel et al., 2016). It is further proposed that the organization of functional interactions may be modulated even by a small perturbation of the regional neurotransmitter concentrations (Suárez et al., 2020). However, one central aspect that has yet to be elucidated is to what extent and how the regional neurotransmitter activity contributes to the rsFC across anatomically separated brain regions.

The regional concentration of the excitatory neurotransmitter glutamate (Glu) and the inhibitory neurotransmitter γ-aminobutyric acid (GABA) can be noninvasively assessed in vivo by magnetic resonance spectroscopy (MRS). MRS-measured Glu and GABA levels can index glutamatergic and GABAergic activity within the investigated regions (Donahue, Near, Blicher, & Jezzard, 2010; Martínez-Maestro, Labadie, & Möller, 2019; Takado et al., 2021). Given the glutamatergic dominance in the long-range cortico-cortical projections (Felleman & Essen, 1991; Markov et al., 2013; Shipp, 2007) and the local tuning and inhibitory role of the GABAergic neurons on the glutamatergic neurons (Buzsáki, Kaila, & Raichle, 2007; Logothetis & Panzeri, 2013), it can be hypothesized that the MRS-measured Glu levels reflect the excitatory glutamatergic activity that is driving the cortico-cortical functional connections, while the MRS-measured GABA levels reflect the local inhibitory GABAergic activity on these long-range cortico-cortical connections. Current evidence from multimodal resting-state functional magnetic resonance imaging (rsfMRI)-MRS studies indicates that there is an association between functional and metabolic measures (Arrubla, Tse, Amkreutz, Neuner, & Shah, 2014; Duncan et al., 2013; Duncan, Enzi, Wiebking, & Northoff, 2011; Enzi et al., 2012; Horn et al., 2010; Kapogiannis, Reiter, Willette, & Mattson, 2013; Levar, Van Doesum, Denys, & Van Wingen, 2019; Newman et al., 2020). Duncan and colleagues concluded that the rsFC between regions, especially within the default mode network (DMN), is positively correlated with the Glu level and negatively correlated with the GABA level in the investigated DMN MRS voxel (Duncan, Wiebking, & Northoff, 2014). However, the generalized hypothesis of a region-independent relationship between local neurotransmitter levels and rsFC was challenged by rsfMRI-MRS studies focusing on

regions outside the DMN, such as the left dorsal and left ventral lateral prefrontal cortex (Wang et al., 2020).

Existing rsfMRI-MRS studies focused on the association of regional Glu or GABA levels and rsFC between two regions mostly in predefined canonical networks. The heterogeneity in the literature regarding the relationship between regional neurotransmitter levels and rsFC (Martens et al., 2020; Passow et al., 2015) suggests that analyses based on single-link rsFCs are not sufficient to reveal a stable general pattern. This, however, can be achieved by an analysis that examines the association between rsFC and regional metabolite levels by varying *rsFC strengths* at the whole-brain level as the strength of rsFC might index underlying neuronal coupling (Pijnenburg et al., 2019; Wilson, Yang, Gore, & Chen, 2016) rooted in regional neurotransmitter activity. Moreover, previous test–retest reliability studies reported poor consistency of the rsFC between two regions at the individual level (Noble, Scheinost, & Constable, 2019), whereas the whole-brain rsFC profile has been proposed to be more stable and robust across multiple scans and imaging sessions (Pannunzi et al., 2017; Shehzad et al., 2009; Takagi, Hirayama, & Tanaka, 2019). Furthermore, a recent study demonstrated that the whole-brain rsFC profile of the respective seed region could robustly predict its regional Glu level (Martens et al., 2020).

In the current study, we examined the overall rsFC profiles of two neighboring cingulate cortex regions, known as the pregenual anterior cingulate cortex (pgACC) and the anterior mid-cingulate cortex (aMCC) that differ in cytoarchitecture, chemoarchitecture and function (Dou et al., 2013; Menon, 2015; Palomero-Gallagher, Vogt, Schleicher, Mayberg, & Zilles, 2009; van Heukelum et al., 2020; Yu et al., 2011). The pgACC is part of the DMN, while the aMCC belongs to the salience network. With the ultra-high field rsfMRI-MRS imaging, we investigated the association between regional neurotransmitter levels and rsFC by varying functional connectivity strengths. We hypothesized that the glutamatergic and GABAergic *edge weights*, which are defined as the degree of the linear association between regional neurotransmitter levels and rsFCs, vary according to the strength of functional connections (*rsFC strength*) in healthy participants. Based on the previous studies, we hypothesized that glutamatergic *edge weights* show a positive linear association with rsFC strengths at the whole-brain level, while GABAergic *edge weights* show a negative correlation. Furthermore, a similar relationship between *rsFC strength* and *edge weights* was expected in both the pgACC and aMCC.

2 | METHODS

2.1 | Participants

One hundred twenty-one healthy participants (mean age ± standard deviation [SD] = 27.2 ± 6.7 years, 45 women) were assessed with the mini-international neuropsychiatric interview (MINI, German Version 5.0.0) to ensure the absence of psychiatric disorders (Ackenheil et al., 1999). Medical history was acquired and confirmed by a study

physician. All participants did not show any psychiatric or neurological diseases and were medication-free (with the exception of contraception pills) determined by their medical history. Further exclusion criteria were pregnancy, left-handedness and MRI contraindications.

All participants gave written informed consent and received financial reimbursement. This study was conducted according to the Declaration of Helsinki and was approved by the Institutional Review Board of the Otto-von-Guericke-University Magdeburg, Germany.

2.2 | Magnetic resonance data acquisition

All participants underwent structural MRI, MRS, and rsfMRI scans in the same session. Participants were scanned following the same protocol order, first the structural scan, then the MRS scans and the rsfMRI, followed by further task-based fMRI scans unrelated to this study. Scanning parameters were as follows: for high-resolution T1-weighted MRI scan: 3D magnetization prepared rapid gradient echo (MPRAGE) sequence, echo time (TE) 2.73 ms, repetition time (TR) 2,300 ms, inversion time (TI) 1,050 ms, flip angle 7°, bandwidth 140 Hz/pixel, acquisition matrix $320 \times 320 \times 224$, isometric voxel size 0.8 mm^3; for rsfMRI scan: echo-planar imaging (EPI) sequence, 280 time points, TE 22 ms, TR 2800 ms, flip angle 80°, FOV 21.2 cm $\times$ 21.2 cm, in-plane isometric voxel size 2 mm, 62 axial slices; for ^{1}H spectra acquisition: stimulated-echo acquisition mode (STEAM) sequence, TE 20 ms, TR 3000 ms, mixing time (TM) 10 ms, bandwidth 2,800 Hz, number of excitations 128. Spectra were acquired with a $20 \times 15 \times 10$ mm^3 voxel in the pgACC (Figure 1a) and with a $25 \times 15 \times 10$ mm^3 voxel in the aMCC (Figure 1b). A single-average water signal served as the internal reference for quantification and eddy-current correction. The positioning of the two MRS voxels that followed anatomical landmarks is described in previous papers from our group (Dou et al., 2013; Dou et al., 2015).

2.3 | Spectroscopy data preprocessing

Spectral data (0.6–4.0 ppm) were fitted and quantified using LCModel (V6.3.0; Stephen Provencher, Inc., Oakville, Canada) (Provencher, 2001) with a sequence-specific basis set. The basis set was measured in the same scanner and included creatine (Cr), Glu, myo-inositol, lactate, N-acetylaspartate (NAA), phosphocholine, taurine, aspartate, GABA, glutamine (Gln), glucose, alanine, N-acetyl-aspartyl-glutamate, phosphocreatine, scyllo-inositol, acetate, succinate, phosphorylethanolamine, glutathione, citrate, and glycerophosphocholine. Spectra were excluded based on visual inspection of the curve fitting and the following objective criteria: Cramér Rao lower bounds (CRLB) > 20%, line width of the magnitude signal>24 Hz, or signal-to-noise ratio (SNR) < 20. Glu, GABA, total Cr (tCr) and NAA were used in the subsequent analyses. An exemplary pgACC spectrum is shown in Figure 1c. The correlation between Glu and GABA was examined using Spearman correlation in both the pgACC and aMCC.
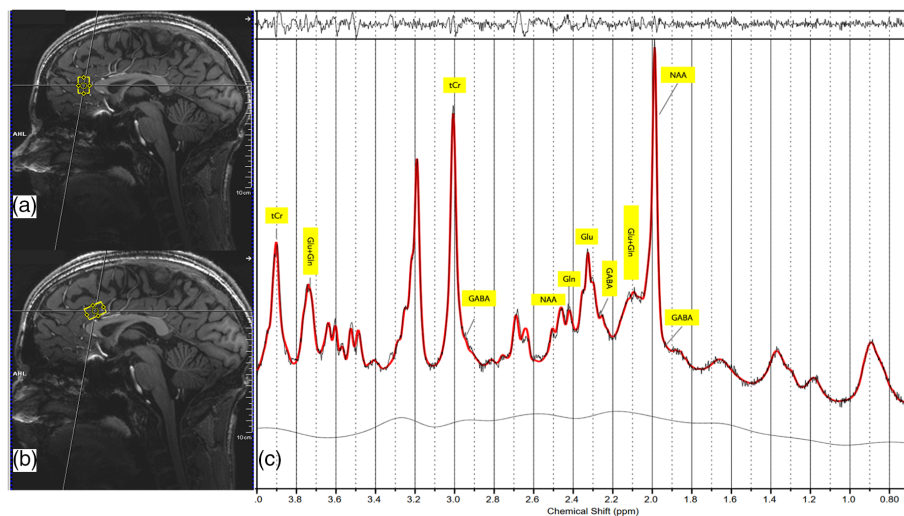
FIGURE 1   Voxel placement for the MRS measurement in the (a) pgACC and (b) aMCC. As shown in the study by Dou et al. (2013), the pgACC voxel was placed touching the genu of the corpus callosum while bypassing the callosomarginal artery, the bottom of the voxel tilting into the AC–PC plane, oriented using the sagittal projection line. For the aMCC, the center of the voxel is projected to the posterior border of the genu of the corpus callosum, along the foot–head direction touching the border of the upper limits of the corpus callosum. (c) Example of a fitted spectral curve using LCModel. AC-PC, anterior commissure–posterior-commissure; aMCC, anterior mid-cingulate cortex; GABA, gamma-aminobutyric acid; Gln, glutamine; Glu, glutamate; MRS, proton magnetic resonance spectroscopy; NAA, N-acetylaspartate; pgACC, pregenual anterior cingulate cortex; tCr, total creatine

2.4 | Structural and functional MRI data preprocessing

Preprocessing of structural and functional MRI data was performed using fMRIPrep 20.1.1 (Esteban et al., 2019), which is based on Nipype 1.5.0 (Gorgolewski et al., 2011), Nilearn 0.6.2 (Abraham et al., 2014) and xcpEngine 1.2.2 (Ciric et al., 2017).

In brief, for each participant, the T1-weighted (T1w) images were corrected for intensity nonuniformity and used as T1w-reference throughout the workflow. The skull-stripped T1w-reference was normalized into the standard space (which is defined by the ICBM 152 Nonlinear Asymmetrical template version 2009c) through nonlinear registration with antsRegistration and segmented into cerebrospinal fluid (CSF), white matter (WM), and gray matter (GM). The nonlinear transformation for the spatial normalization was saved and further applied on the pgACC and aMCC MRS voxels. Then, the following preprocessing was performed for the acquired rsfMRI images. A reference volume and its skull-stripped version were generated and co-registered to the T1w reference. The BOLD images were slice-time corrected and the head-motion parameters with respect to the BOLD reference (transformation matrices and six corresponding rotation and translation parameters) were estimated. Confounding time-series of frame-wise displacement (FD) and DVARS (D temporal derivative of time courses, VARS referring to RMS variance over voxels) (Power, Barnes, Snyder, Schlaggar, & Petersen, 2012) were calculated and region-wise averaged signals (within the CSF and WM) were extracted with the help of the segmented T1w. Frames that exceeded a threshold of 0.5 mm FD or 1.5 standardized DVARS

were annotated as motion outliers. Participants with excessive head motions, defined by a mean FD threshold > 0.25 mm over all volumes during EPI scans, were excluded. With the preprocessed BOLD images from fMRIPrep, xcpEngine was employed to perform the nuisance regression for head motion and physiological signals. Based on the benchmarking of 14 participant-level confounds regression strategies for controlling motion artifact predefined in xcpEngine, the denoising strategy 36P + SPKREG adapted from Satterthwaite et al. (Satterthwaite et al., 2013) was applied. Prior to the confounds regression, the same temporal filter (0.01–0.08 Hz) was applied to both the preprocessed rsfMRI data and the confounds time series (avoiding re-introduction of filtered frequencies) (Hallquist, Hwang, & Luna, 2013). Finally, data were visually inspected by two independent raters to exclude abnormalities of anatomical segmentation and functional normalization.

2.5 | Functional connectivity profiles and rsFC strengths

The rsFC seeds for the pgACC and aMCC matched the MRS voxel placement for each participant. A binary mask was created based on the placement of the MRS voxel with the native T1w as the structural reference and subsequently normalized into the same standard space as the functional processed images. To characterize the rsFC profile, the atlas of Schaefer2018_400Parcels_7Networks (Schaefer et al., 2018) was applied to parcellate the cortex into 400 regions in MNI space. Subsequently, the averaged time courses of these 400 parcellated regions and the pgACC and aMCC

MRS seeds were extracted. For each participant, rsFCs were calculated as Pearson correlation coefficients between the pgACC and aMCC and the 400 parcellated regions. Then Fisher Z transformation was performed with the calculated rsFC. The resulting rsFC profile of each region was characterized by identifying brain parcels that showed a statistically significant rsFC to the pgACC or aMCC at the group level (one-sample t-test with the adjusted p value (Bonferroni correction, $p < .05/200$, the threshold of 200 was chosen due to the symmetry of the left and right hemispheres). Parcels belonging to the DMN were investigated separately in an exploratory manner.

The *rsFC strengths* were calculated as group mean rsFCs between the seed regions and parcels across participants. Parcels with a *rsFC strength* larger than the mean ± 2 *SD* across participants were labeled as outliers and removed from further analysis.

2.6 | Glutamatergic and GABAergic edge weights

The *glutamatergic* and *GABAergic edge weights* were defined as the across-participants partial correlation coefficients between the pgACC and aMCC metabolite levels (Glu or GABA) and the rsFC of the pgACC or aMCC to each target parcel, controlling for age, sex, the proportion of the CSF within the investigated MRS voxel, control metabolite and the mean rsFC between the pgACC or aMCC and all parcels (See Figure 2 for an overview). Here, the mean rsFC was controlled since it can reduce positive biases when the global signal regression is not performed for the rsFC calculation (Glasser et al., 2018; Smith et al., 2011). Glu served as the control metabolite for GABA, and vice versa, in the primary analysis (Wang et al., 2020). Additional tests were done with tCr and NAA as control metabolites or without control metabolites (reported in Table S1). The Shapiro–
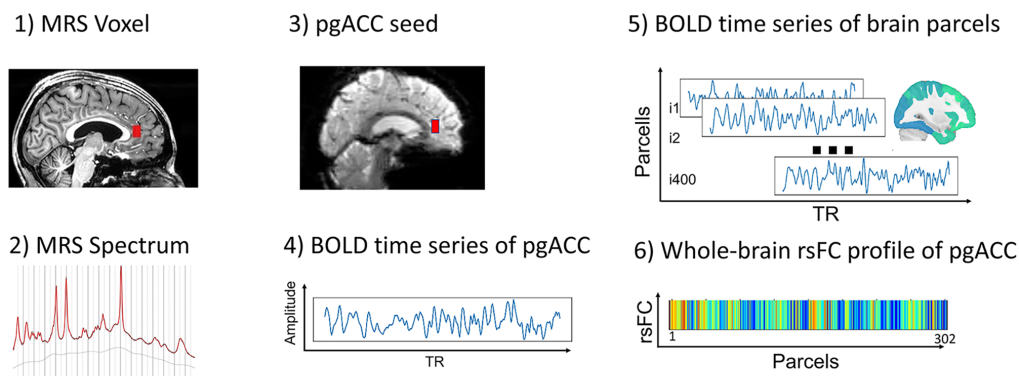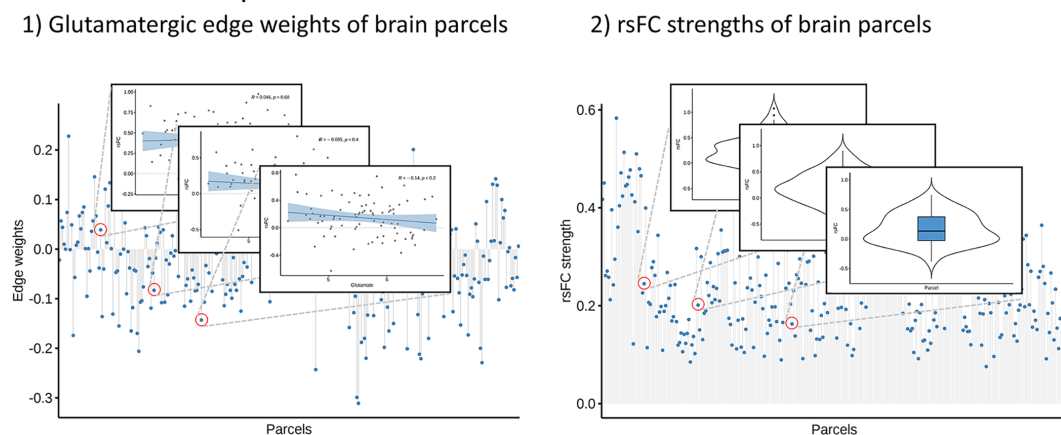

FIGURE 2 Overview of the analysis pipeline on (a) the participant-level and (b) across-participants for the pgACC. (a) MRS-Spectra were acquired with a 20 × 15 × 10 mm³ voxel in the pgACC (in red [a1]). Spectral data were fitted and quantified using LCModel (a2). The rsFC seed for the pgACC matched the MRS voxel placement for each participant (a3) and the average time course was extracted (a4). The averaged time series of brain parcels from the atlas of Schaefer2018_400Parcels_7Networks (Schaefer et al., 2018) were extracted (a5) and rsFCs between the pgACC and 400 brain parcels were calculated via Pearson correlation. The rsFC profile was characterized by identifying brain parcels that showed a statistically significant rsFC to the pgACC (a6). (b) The glutamatergic edge weights were calculated for each brain parcel via across-participants partial correlation between the pgACC metabolite levels and the rsFC of the pgACC to each target parcel (b1). The rsFC strength per parcel was calculated as a group mean rsFC (b2) between pgACC and that parcel. BOLD, blood oxygenation level dependent; GABA, gamma-aminobutyric acid; Glu, glutamate; MRS, magnetic resonance spectroscopy; pgACC, pregenual anterior cingulate cortex; rsFC, resting-state functional connectivity

Wilk test was applied to examine whether the metabolite concentrations were normally distributed or not. When the normal distribution assumption was violated, partial Spearman correlation was applied instead of Pearson partial correlation for the definition of the *glutamatergic* and *GABAergic edge weights*.

2.7 | Statistical analysis

Pearson correlation was used to test the associations between the pgACC or aMCC *glutamatergic* or *GABAergic edge weights* and *rsFC strengths* across brain parcels. The statistical threshold was Bonferroni corrected for two MRS voxels and two metabolites that were investigated ($p < .0125$).

All statistical analyses were performed using Python (version 3.6.8) with Pandas and NumPy, as well as the statistical package of Pingouin (version 0.3.10; Vallat, 2018). The figures were created using R (version 4.0.3) and the package ggpubr (version 0.4.0).

3 | RESULTS

3.1 | Sample characteristics and metabolites

Demographic and metabolite data are shown in Table 1. The number of included participants for the investigated metabolites varied between the pgACC and aMCC, due to the quality criteria for the measured metabolites that were applied on each voxel separately. Moreover, participants were excluded from the analysis if they exceeded a motion threshold during rsfMRI. This led to inclusion of 81 participants for the pgACC analyses and 76 participants for the aMCC analyses out of initial 121 participants.

TABLE 1 Sample characteristics and magnetic resonance spectroscopy measures of metabolites in the pgACC and aMCC (expressed as number, mean or percentage [*SD*])

		pgACC	aMCC
N (f/m)		81 (34/47)	76 (30/46)
Age (years)		27.4 (7.0)	27.9 (7.4)
SNR		45.4 (6.0)	44.3 (5.4)
FWHM (ppm)		0.019 (0.007)	0.015 (0.005)
nonCSF (%)		93.1 (4.5)	95.6 (4.5)
CRLB (%)	Glu	2.9 (0.8)	2.7 (0.6)
	GABA	8.9 (2.1)	9.1 (2.6)
Conc (i.u.)	Glu	5.6 (0.6)	5.8 (0.3)
	GABA	1.6 (0.4)	1.7 (0.5)

Abbreviations: aMCC, anterior mid-cingulate cortex; Conc (i.u.), concentration (institutional units); CRLB, Cramer-Rao Lower Bound; CSF, cerebrospinal fluid; f/m, female/male; FWHM, full-width half-maximum in parts per million (ppm); GABA, gamma-aminobutyric acid; Glu, glutamate; *N*, number; pgACC, pregenual anterior cingulate cortex; SNR, signal-to-noise ratio.

Except aMCC GABA ($W = 0.94$, $p = .001$), metabolites were normally distributed (pgACC: Glu, $W = 0.98$, $p = .326$; GABA, $W = 0.97$, $p = .052$; aMCC: Glu, $W = 0.99$, $p = .623$). In both investigated MRS voxels, Glu and GABA were significantly correlated (pgACC: $r = 0.27$, CI 95% = [0.05, 0.46], $n = 81$, $p = .016$; aMCC; $r = 0.42$, CI 95% = [0.22, 0.59], $n = 76$, $p < .001$).

3.2 | Relationship between glutamatergic and GABAergic edge weights and whole-brain pgACC rsFC strengths

The pgACC rsFC profile included 302 parcels. The *rsFC strengths* between the pgACC and its parcels were positively correlated with the glutamatergic *edge weights* ($r = .33$, CI 95% = [0.23, 0.43], $p < .001$; Figure 3a). A positive correlation between the *rsFC strengths* and the GABAergic *edge weights* was also found ($r = .18$, CI 95% = [0.07, 0.29], $p < .001$; Figure 3b). Additional analyses (including NAA and tCr as control metabolites and without control metabolites) showed the same associations (except the tCr as control metabolite for the Glu in aMCC) and the results are shown in Table S1.

To replicate previous findings within the DMN, the same analyses were repeated, this time limiting the rsFC profile of the pgACC to brain parcels within the DMN (n_parcels = 76). The *rsFC strengths* between DMN parcels and the pgACC showed a significant positive correlation with the glutamatergic *edge weights* ($r = .44$, CI 95% = [0.24, 0.61], $p < .001$) but not with GABAergic *edge weights* ($r = -.07$, CI 95% = [−0.29, 0.16], $p = .56$).

3.3 | Relationship between glutamatergic and GABAergic edge weights and whole-brain aMCC rsFC strengths

The aMCC rsFC profile included 334 parcels. A significant negative correlation was found between the glutamatergic *edge weights* and the *rsFC strengths* across these parcels ($r = −.14$, CI 95% = [−0.25, −0.04], $p = .004$; Figure 4a). The GABAergic *edge weights* were also negatively correlated with the *rsFC strengths* ($r = −.28$, CI 95% = [−0.38, −0.18], $p < .001$; Figure 4b). Results of the exploratory analysis, controlling for different metabolites (including NAA and total Cr) or using no control metabolite were similar (Table S1).

When constraining the rsFC profile to the DMN (n_parcels = 69), a trend-level negative correlation was found between the glutamatergic *edge weights* and *rsFC strengths* between the aMCC and the DMN parcels ($r = −.27$, CI 95% = [−0.48, −0.04], $p = .023$). In contrast, no significant correlation was found between the GABAergic *edge weights* and *rsFC strengths* ($r = −0.12$, CI 95% = [−0.35, 0.12], $p = .31$).

4 | DISCUSSION

Using multimodal ultra-high field MR imaging in a large sample of healthy participants, we examined the association of *rsFC strengths*
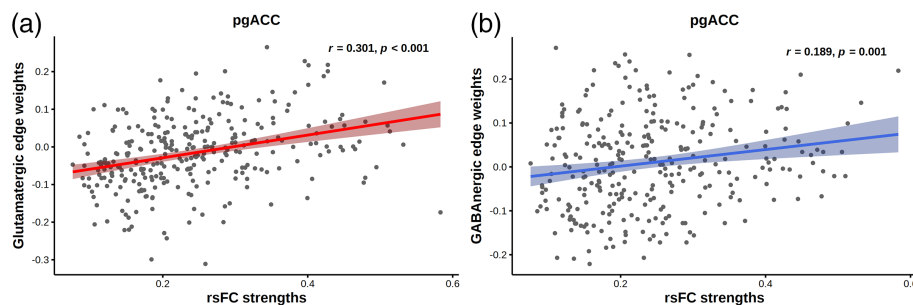
FIGURE 3 Scatterplot of (a) glutamatergic and (b) GABAergic edge weights and rsFC strengths in the pgACC. Each dot represents one parcel. Shaded areas represent 95% CIs. Glutamatergic and GABAergic edge weights correspond to the partial correlation coefficients between the local metabolite levels and the rsFC of the pgACC to a given brain parcel. GABA, gamma-aminobutyric acid; Glu, glutamate; pgACC, pregenual anterior cingulate cortex; rsFC, resting-state functional connectivity
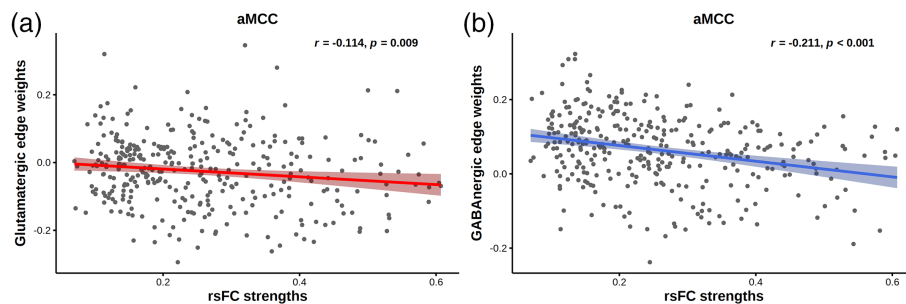

FIGURE 4 Scatterplot of (a) glutamatergic and (b) GABAergic edge weights and rsFC strengths in the aMCC. Each dot represents one parcel. Shaded areas represent 95% confidence intervals. Glutamatergic and GABAergic edge weights correspond to the partial correlation coefficients between the local metabolite levels and the rsFC of the aMCC to a given brain parcel. aMCC, anterior mid-cingulate cortex; GABA, gamma-aminobutyric acid; Glu, glutamate; rsFC, resting-state functional connectivity

with the glutamatergic and GABAergic *edge weights* in two neighboring but distinct cingulate cortex subdivisions. Our results support the hypothesized linkage of regional neurotransmitter levels and the strength of rsFC across brain parcels at the whole-brain level. We hypothesized that the *rsFC strengths* of both cingulate cortex regions to their functionally connected brain parcels would correlate positively with glutamatergic and negatively with GABAergic *edge weights*. On the contrary, our results showed a region-dependent relationship robust to the effects of age, sex and local levels of control metabolites. Specifically, both glutamatergic and GABAergic *edge weights* were positively correlated with the *rsFC strengths* of the pgACC, while both *edge weights* were negatively correlated with the *rsFC strengths* of the aMCC. Our results indicate that the contribution of Glu and GABA levels to the rsFC profile might differ between brain regions at rest.

We hypothesized opposite directionality of the association between the glutamatergic and GABAergic *edge weights* and *rsFC strengths*, based on the findings of previous rsfMRI-MRS studies (Duncan et al., 2014; Kapogiannis et al., 2013) and also considering the distinct physiological effect of excitatory and inhibitory neurotransmitters. However, the present findings showed that glutamatergic and GABAergic *edge weights* correlate with *rsFC strengths* in a similar manner. Here, it is important to differentiate the *edge*

weights, which represent the magnitude of the linear association between the rsFC and regional Glu or GABA levels across subjects and the association between *edge weights* and *rsFC strengths* across brain parcels, with the *rsFC strength* being defined as the group mean rsFC between the selected cingulate cortex subregions and a particular brain parcel. As shown in Figures 3 and 4, there were both positive and negative glutamatergic or GABAergic *edge weights* between the selected cingulate cortex regions and brain parcels. It is therefore plausible that the regional Glu and GABA levels are associated with the rsFC between the selected cingulate cortex subregions and certain brain parcels in an opposite manner, while still showing a similar whole-brain linear direction. Indeed, the heterogeneity found in the literature indicates that the choice of seed regions in rsfMRI analyses influences the reported association patterns. For example, several studies did not find any significant association between the rsFC and regional Glu (Levar et al., 2019; Passow et al., 2015) or GABA levels (Martens et al., 2020; Stagg et al., 2014), while some reported a significant positive correlation of regional GABA levels with the rsFC (Levar et al., 2019).

By examining the association between regional metabolite levels and the whole-brain rsFC profile of the seed regions, our study shows the potential to characterize the relationship between regional neurotransmitter levels and overall functional connectivity of the

investigated regions. Our findings indicate that glutamatergic or GABAergic *edge weights* in the pgACC tend to increase with increasing *rsFC strengths*, while the glutamatergic and GABAergic *edge weights* tend to decrease with increasing *rsFC strengths* in the aMCC. Stronger rsFCs might reflect underlying anatomical connections (Wang et al., 2013), as well as neuronal coupling (Pijnenburg et al., 2019; Wilson et al., 2016), while the remaining nonzero rsFCs may root from observational noises or unobserved common-inputs (Stevenson, Rebesco, Miller, & Körding, 2008) underlying the statistical dependency between the BOLD activities of two investigated brain regions. Our findings, linear but distinctive association between metabolites and rsFC along with the varying *rsFC strengths*, suggest a differential contribution of local neurotransmitter activity to cortico-cortical functional connections in the pgACC and aMCC at rest. The examination at the whole-brain level enabled us to shed some light on the relationship between neurotransmitter activity at the microscale level and functional connectivity at the macroscale level within the spatial and temporal limitations of MRS and rsFC. Future studies combining effective connectivity measures and multi voxel magnetic resonance spectroscopic imaging (MRSI) at rest as well as functional magnetic resonance spectroscopy of the brain (fMRS) are needed to understand the relationship between local neurotransmitter activity and long-range cortico-cortical projections.

The region-dependent association in the two investigated cingulate cortex subdivisions may root in their differences at the microscale and the macroscale levels. These two neighboring cingulate cortex regions differ not only in cyto- and receptor architecture (Palomero-Gallagher et al., 2009) but also in their structural and functional connectivity profile (van Heukelum et al., 2020; Yu et al., 2011). At the microscale level, with regard to receptor architecture, the pgACC is richer in metabotropic GABA-B and α-amino-3-hydroxy-5-methyl-4-isoxazolepropionic acid (AMPA) receptors, while the aMCC is relatively rich in ionotropic GABA-A and *N*-methyl-D-aspartate (NMDA) receptors (Palomero-Gallagher et al., 2009). The distinction in structure and function at both the microscale and macroscale levels also shows itself in the distinctive roles of the pgACC and aMCC in cognition and emotion (Stevens, 2011; van Heukelum et al., 2020). The pgACC, as part of the DMN, is involved in self-related cognitive processes and its activity typically decreases when performing stimulus-driven tasks (Greicius et al., 2003). It is furthermore one of the key nodes of the affective network and part of the visceromotor system, therefore the pgACC shows a high functional connection to brain regions processing emotional stimuli (Pizzagalli, 2011) and is also involved in the control of the autonomic nervous system (Thayer, Åhs, Fredrikson, Sollers III, & Wager, 2012). In contrast, the aMCC is one of the major constituents of the salience network (Menon, 2015). It is involved in attention and action control and its activation inhibits goal-unrelated brain activity (Spielberg, Miller, Heller, & Banich, 2015) or exerts an inhibitory influence on the DMN regions (Zhou et al., 2018).

Considering the broad interest in the associations of regional GABA and Glu with rsFC within the DMN (Duncan et al., 2014; Gonen et al., 2020; Kapogiannis et al., 2013; Passow et al., 2015), we repeated our analyses by limiting the *rsFC strengths* of the pgACC and aMCC to brain parcels within the DMN. We found that the glutamatergic *edge weights* were positively correlated with the *rsFC strengths* of the pgACC to the DMN regions, while there was no significant correlation for the GABAergic *edge weights*. This exploratory analysis supported the previously reported across subjects positive linear association between the regional Glu levels and the rsFC within the DMN (Duncan et al., 2011; Duncan et al., 2013; Enzi et al., 2012; Kapogiannis et al., 2013). Contrary to some previous findings on an across subjects level (Arrubla et al., 2014; Duncan et al., 2014; Kapogiannis et al., 2013), there was no negative correlation between the regional GABA levels and *rsFC strengths* within the DMN in our study. The negative correlation between the glutamatergic *edge weights* and the *rsFC strengths* of the aMCC to the DMN regions did not reach the adjusted significance level. There was no statistically significant correlation of the GABAergic *edge weights* with the DMN *rsFC strengths* in the aMCC, either. These findings suggest that the contribution of local neurotransmitter levels to rsFC within- and between- brain networks differs at rest.

It is important to note that most of the previous rsfMRI-MRS studies measured either Glu or GABA. It is challenging to integrate the effects of different metabolites from separate studies considering the spectral editing techniques that might be centered on GABA by overly suppressing the Glu signal. Moreover, most of the studies measured Glx (pooled Glu, Gln, and GABA) as a surrogate marker of glutamatergic activity due to technical difficulties in resolving Glu from Gln and GABA at lower field strengths. With the increased spectral dispersion at an ultra-high field, the increased ability to assess Glu and GABA from the same measurement session provides a more reliable assessment of the association of these neurotransmitters with rsFC in the same individuals. Additionally, the validity of the applied measurement strategy in this study has been investigated (Dou et al., 2015), particularly in the human cingulate cortex subregions (Dou et al., 2013).

5 | LIMITATIONS

Several limitations were taken into consideration and, where possible, addressed to the best of our knowledge. First, the MRS voxels were placed individually for each participant to avoid signal contamination in the pgACC voxel by the callosomarginal artery, or in the aMCC voxel by the callosal branches. To minimize the variation of placements, the MRS voxels were placed by the same experienced technician (R.B.L.), who has participated in multiple studies involving MRS measurements focusing on the pgACC and aMCC during the past decade. Second, diurnal fluctuations may affect the glutamatergic system and rsFC, at least the rsFC of the DMN (Fafrowicz et al., 2019; Jiang et al., 2016; Shannon et al., 2012). To minimize the effects of the time of the day, all participants were scanned between 10.30 a.m. and 4.30 p.m. The present study also relied on the validity of the glutamatergic measures at 7 T with short TE MRS, while those at 3 T utilize intermediate or long TEs. Therefore, in the context of

generalizability, the reported findings and their translation to other studies need to be done with caution, especially for studies at lower field strengths. Lastly, besides their function in phasic inhibition and excitation during neurotransmission, GABA and Glu serve multiple other functions, such as the regulation of tonic inhibition and excitation (Stagg et al., 2009), the regulation of metabolism (Albrecht, Sidoryk-Węgrzynowicz, Zielińska, & Aschner, 2010; Bak, Schousboe, & Waagepetersen, 2006; Hertz & Rothman, 2016) and the shaping of cortical functional architecture (Kolasinski et al., 2017; Puts, Edden, Evans, McGlone, & McGonigle, 2011; Robertson, Ratai, & Kanwisher, 2016). Moreover, the temporal (averaged signal over the acquisition time) and spatial resolution (e.g., $20 \times 15 \times 10 \text{ mm}^3$ or $25 \times 15 \times 10 \text{ mm}^3$ voxel size) of MRS is relatively low considering that neurotransmission takes place at a nanometer scale within milliseconds. It is therefore difficult to draw direct conclusions about mechanisms exclusively attributed to the neurotransmission within the seed area and the associated *rsFC strengths*.

6 | CONCLUSION

With the ultra-high field rsfMRI-MRS measurements, we investigated the association between the regional Glu and GABA levels measured in the pgACC and aMCC and their whole-brain rsFC profiles. Instead of a region-independent association, our results indicate a region-dependent association of glutamatergic and GABAergic *edge weights* and *rsFC strengths*. Our results highlight the complex relationship between regional neurotransmitter levels and the rsFC that does not follow basic assumptions of the physiological roles of neurotransmitters at the cellular level. More studies mapping metabolites in multiple regions (e.g., with volumetric proton MRSI; Maudsley et al., 2009) are warranted to further elucidate metabolite and network specific interactions and their role in brain organization.

CONFLICT OF INTERESTS
Martin Walter is a member of the advisory boards and gave presentations for the following companies: Boehringer Ingelheim, Germany; Bayer AG, Germany; and Biologische Heilmittel Heel GmbH, Germany. Martin Walter has further conducted studies with institutional research support from HEEL and from Janssen Pharmaceutical Research for a clinical trial (IIT) on ketamine in patients with major depression unrelated to this investigation. Martin Walter has not received any financial compensation from above-mentioned companies. All other authors report no biomedical financial interests or potential conflicts of interest.

AUTHOR CONTRIBUTIONS
Meng Li preprocessed and analyzed the data, interpreted the findings, and wrote the manuscript. Zümrüt Duygu Sen and Martin Walter designed and conceptualized the study, interpreted the findings and revised the manuscript. Lena Vera Danyeli and Lejla Colic were involved in the preprocessing and analysis of the study, interpreted the findings, and revised the manuscript. Gerd Wagner, Stefan Smesny, Tara Chand, Xin Di, Bharat B. Biswal, Jörn Kaufmann, Jürgen R. Reichenbach, and Oliver Speck assisted in the analysis and interpretation of data and revised the manuscript. All authors contributed to the article and approved the submitted version.

DATA AVAILABILITY
The datasets generated for this study are available from the corresponding author upon reasonable request.

ORCID
Meng Li https://orcid.org/0000-0002-7423-0090
Lejla Colic https://orcid.org/0000-0002-8809-4034
Gerd Wagner https://orcid.org/0000-0003-2296-0259
Xin Di https://orcid.org/0000-0002-2422-9016
Bharat B. Biswal https://orcid.org/0000-0002-3710-3500
Jürgen R. Reichenbach https://orcid.org/0000-0002-2640-0630
Oliver Speck https://orcid.org/0000-0002-6019-5597
Zümrüt Duygu Sen https://orcid.org/0000-0001-8246-5650

REFERENCES
Abraham, A., Pedregosa, F., Eickenberg, M., Gervais, P., Mueller, A., Kossaifi, J., ... Varoquaux, G. (2014). Machine learning for neuroimaging with scikit-learn. *Frontiers in Neuroinformatics*, 8, 8. https://doi.org/10.3389/fninf.2014.00014/full

Ackenheil, M., Stotz, G., Dietz-Bauer, R., Vossen, A., Dietz, R., Vossen-Wellmann, A., & Vossen, J. (1999). *Deutsche Fassung des mini-international neuropsychiatric interview*. München: Psychiatrische Universitätsklinik München. https://www.semanticscholar.org/paper/Deutsche-Fassung-des-Mini-International-Interview-Ackenheil-Stotz/5d22ddb5d4216d32b4070db5e15ab3df4f909b6d

Albrecht, J., Sidoryk-Węgrzynowicz, M., Zielińska, M., & Aschner, M. (2010). Roles of glutamine in neurotransmission. *Neuron Glia Biology*, 6, 263–276.

Allan, T. W., Francis, S. T., Caballero-Gaudes, C., Morris, P. G., Liddle, E. B., Liddle, P. F., ... Gowland, P. A. (2015). Functional connectivity in MRI is driven by spontaneous BOLD events. *PLoS One*, 10, e0124577.

Amunts, K., & Zilles, K. (2015). Architectonic mapping of the human brain beyond Brodmann. *Neuron*, 88, 1086–1107.

Arrubla, J., Tse, D. H. Y., Amkreutz, C., Neuner, I., & Shah, N. J. (2014). GABA concentration in posterior cingulate cortex predicts putamen response during resting state fMRI. *PLoS ONE*, 9, e106609.

Bak, L. K., Schousboe, A., & Waagepetersen, H. S. (2006). The glutamate/GABA-glutamine cycle: Aspects of transport, neurotransmitter homeostasis and ammonia transfer. *Journal of Neurochemistry*, 98, 641–653.

Biswal, B., Yetkin, F. Z., Haughton, V. M., & Hyde, J. S. (1995). Functional connectivity in the motor cortex of resting human brain using echo-planar MRI. *Magnetic Resonance in Medicine*, 34, 537–541.

Burke, K. J. J., & Bender, K. J. (2019). Modulation of ion channels in the axon: Mechanisms and function. *Frontiers in Cellular Neuroscience*, 13, 221. https://doi.org/10.3389/fncel.2019.00221/full

Buzsáki, G., Kaila, K., & Raichle, M. (2007). Inhibition and brain work. *Neuron*, 56, 771–783.

Ciric, R., Wolf, D. H., Power, J. D., Roalf, D. R., Baum, G. L., Ruparel, K., ... Satterthwaite, T. D. (2017). Benchmarking of participant-level confound regression strategies for the control of motion artifact in studies of functional connectivity. *Neuroimage*, 174–187.

Damoiseaux, J. S., Rombouts, S., Barkhof, F., Scheltens, P., Stam, C. J., Smith, S. M., & Beckmann, C. F. (2006). Consistent resting-state networks across healthy subjects. *Proceedings of the National Academy of Sciences*, 103, 13848–13853.

De Luca, M., Beckmann, C. F., De Stefano, N., Matthews, P. M., & Smith, S. M. (2006). fMRI resting state networks define distinct modes of long-distance interactions in the human brain. *NeuroImage*, 29, 1359–1367.

Donahue, M. J., Near, J., Blicher, J. U., & Jezzard, P. (2010). Baseline GABA concentration and fMRI response. *NeuroImage*, 53, 392–398.

Dou, W., Kaufmann, J., Li, M., Zhong, K., Walter, M., & Speck, O. (2015). The separation of Gln and Glu in STEAM: A comparison study using short and long TEs/TMs at 3 and 7 T. *Magnetic Resonance Materials in Physics, Biology and Medicine*, 28, 395–405.

Dou, W., Palomero-Gallagher, N., van Tol, M.-J., Kaufmann, J., Zhong, K., Bernstein, H.-G., ... Walter, M. (2013). Systematic regional variations of GABA, glutamine, and glutamate concentrations follow receptor fingerprints of human cingulate cortex. *Journal of Neuroscience*, 33, 12698–12704.

Duncan, N. W., Enzi, B., Wiebking, C., & Northoff, G. (2011). Involvement of glutamate in rest-stimulus interaction between perigenual and supragenual anterior cingulate cortex: A combined fMRI-MRS study. *Human Brain Mapping*, 32, 2172–2182.

Duncan, N. W., Wiebking, C., & Northoff, G. (2014). Associations of regional GABA and glutamate with intrinsic and extrinsic neural activity in humans—A review of multimodal imaging studies. *Neuroscience & Biobehavioral Reviews*, 47, 36–52.

Duncan, N. W., Wiebking, C., Tiret, B., Marjańska, M., Hayes, D. J., Lyttleton, O., ... Northoff, G. (2013). Glutamate concentration in the medial prefrontal cortex predicts resting-state cortical-subcortical functional connectivity in humans. *PLoS One*, 8, e60312.

Enzi, B., Duncan, N. W., Kaufmann, J., Tempelmann, C., Wiebking, C., & Northoff, G. (2012). Glutamate modulates resting state activity in the perigenual anterior cingulate cortex – A combined fMRI–MRS study. *Neuroscience*, 227, 102–109.

Esteban, O., Markiewicz, C. J., Blair, R. W., Moodie, C. A., Isik, A. I., Erramuzpe, A., ... Gorgolewski, K. J. (2019). fMRIPrep: A robust preprocessing pipeline for functional MRI. *Nature Methods*, 16, 111–116.

Fafrowicz, M., Bohaterewicz, B., Ceglarek, A., Cichocka, M., Lewandowska, K., Sikora-Wachowicz, B., ... Marek, T. (2019). Beyond the low frequency fluctuations: Morning and evening differences in human brai. *Frontiers in Human Neuroscience*, 13, 288. https://doi.org/10.3389/fnhum.2019.00288/full

Felleman, D. J., & Essen, D. C. V. (1991). Distributed hierarchical processing in the primate cerebral cortex. *Cerebral Cortex*, 1, 1–47.

Friston, K. J. (1994). Functional and effective connectivity in neuroimaging: A synthesis. *Human Brain Mapping*, 2, 56–78.

Friston, K. J. (2011). Functional and effective connectivity: A review. *Brain Connectivity*, 1, 13–36.

Glasser M. F., Coalson T.S., Bijsterbosch J.D., Harrison S.J., Harms M.P., Anticevic A., ... Smith S.M. (2018). Using temporal ICA to selectively remove global noise while preserving global signal in functional MRI data. *NeuroImage*, 181, 692–717. http://dx.doi.org/10.1016/j.neuroimage.2018.04.076

Gonen, O. M., Moffat, B. A., Kwan, P., O'Brien, T. J., Desmond, P. M., & Lui, E. (2020). Resting-state functional connectivity and quantitation of glutamate and GABA of the PCC/precuneus by magnetic resonance spectroscopy at 7T in healthy individuals. *PLoS ONE*, 15, e0244491.

Gorgolewski, K., Burns, C. D., Madison, C., Clark, D., Halchenko, Y. O., Waskom, M. L., & Ghosh, S. S. (2011). Nipype: A flexible, lightweight and extensible neuroimaging data processing framework in python. *Frontiers in Neuroinformatics*, 5, 5. https://doi.org/10.3389/fninf.2011.00013/full

Greicius M. (2008). Resting-state functional connectivity in neuropsychiatric disorders. *Current opinion in neurology*, 21(4), 424–430.

Greicius, M. D., Krasnow, B., Reiss, A. L., & Menon, V. (2003). Functional connectivity in the resting brain: A network analysis of the default mode hypothesis. *Proceedings of the National Academy of Sciences*, 100, 253–258.

Hallquist, M. N., Hwang, K., & Luna, B. (2013). The nuisance of nuisance regression: Spectral misspecification in a common approach to resting-state fMRI preprocessing reintroduces noise and obscures functional connectivity. *NeuroImage*, 82, 208–225.

Hertz, L., & Rothman, D. L. (2016). Glucose, lactate, β-hydroxybutyrate, acetate, GABA, and succinate as substrates for synthesis of glutamate and GABA in the glutamine–glutamate/GABA cycle. In A. Schousboe & U. Sonnewald (Eds.), *The glutamate/GABA-glutamine cycle: Amino acid neurotransmitter homeostasis.* (pp. 9–42). Cham: Springer International Publishing. https://doi.org/10.1007/978-3-319-45096-4_2

Horn, D. I., Yu, C., Steiner, J., Buchmann, J., Kaufmann, J., Osoba, A., ... Walter, M. (2010). Glutamatergic and resting-state functional connectivity correlates of severity in major depression – The role of Pregenual anterior cingulate cortex and anterior insula. *Frontiers in Systems Neuroscience*, 4, 1–10.

Jiang, C., Yi, L., Su, S., Shi, C., Long, X., Xie, G., & Zhang, L. (2016). Diurnal variations in neural activity of healthy human brain decoded with resting-state blood oxygen level dependent fMRI. *Frontiers in Human Neuroscience*, 10, 10. https://doi.org/10.3389/fnhum.2016.00634/full

Kapogiannis, D., Reiter, D. A., Willette, A. A., & Mattson, M. P. (2013). Posteromedial cortex glutamate and GABA predict intrinsic functional connectivity of the default mode network. *Neuroimage*, 64, 112–119.

Kolasinski, J., Logan, J. P., Hinson, E. L., Manners, D., Divanbeighi Zand, A. P., Makin, T. R., ... Stagg, C. J. (2017). A mechanistic link from GABA to cortical architecture and perception. *Current Biology*, 27, 1685–1691.e3.

Levar, N., Van Doesum, T. J., Denys, D., & Van Wingen, G. A. (2019). Anterior cingulate GABA and glutamate concentrations are associated with resting-state network connectivity. *Scientific Reports*, 9, 2116.

Logothetis, N. K. (2003). The underpinnings of the BOLD functional magnetic resonance imaging signal. *The Journal of Neuroscience*, 23, 3963–3971.

Logothetis, N. K., & Panzeri, S. (2013). Local field potential, relationship to BOLD signal. In D. Jaeger & R. Jung (Eds.), *Encyclopedia of computational neuroscience.* (pp. 1–11). New York, NY: Springer.

Logothetis, N. K., & Wandell, B. A. (2004). Interpreting the BOLD signal. *Annual Review of Physiology*, 66, 735–769.

Markov, N. T., Ercsey-Ravasz, M., Lamy, C., Gomes, A. R. R., Magrou, L., Misery, P., ... Kennedy, H. (2013). The role of long-range connections on the specificity of the macaque interareal cortical network. *PNAS*, 110, 5187–5192.

Martens, L., Kroemer, N. B., Teckentrup, V., Colic, L., Palomero-Gallagher, N., Li, M., & Walter, M. (2020). Localized prediction of glutamate from whole-brain functional connectivity of the Pregenual anterior cingulate cortex. *The Journal of Neuroscience*, 40, 9028–9042.

Martínez-Maestro, M., Labadie, C., & Möller, H. E. (2019). Dynamic metabolic changes in human visual cortex in regions with positive and

negative blood oxygenation level-dependent response. *Journal of Cerebral Blood Flow and Metabolism*, 39, 2295–2307.

Maudsley, A. A., Domenig, C., Govind, V., Darkazanli, A., Studholme, C., Arheart, K., & Bloomer, C. (2009). Mapping of brain metabolite distributions by volumetric proton MR spectroscopic imaging (MRSI). *Magnetic Resonance in Medicine*, 61, 548–559.

Meir, A., Ginsburg, S., Butkevich, A., Kachalsky, S. G., Kaiserman, I., Ahdut, R., ... Rahamimoff, R. (1999). Ion channels in presynaptic nerve terminals and control of transmitter release. *Physiological Reviews*, 79, 1019–1088.

Menon, V. (2015). Salience network. In A. W. Toga (Ed.), *Brain mapping* (pp. 597–611). Waltham: Academic Press.

Mueller, S., Wang, D., Fox, M. D., Yeo, B. T. T., Sepulcre, J., Sabuncu, M. R., ... Liu, H. (2013). Individual variability in functional connectivity architecture of the human brain. *Neuron*, 77, 586–595.

Newman, S. D., Cheng, H., Kim, D.-J., Schnakenberg-Martin, A., Dydak, U., Dharmadhikari, S., ... O'Donnell, B. (2020). An investigation of the relationship between glutamate and resting state connectivity in chronic cannabis users. *Brain Imaging and Behavior*, 14, 2062–2071.

Noble, S., Scheinost, D., & Constable, R. T. (2019). A decade of test-retest reliability of functional connectivity: A systematic review and meta-analysis. *NeuroImage*, 203, 116157.

Palomero-Gallagher, N., Vogt, B. A., Schleicher, A., Mayberg, H. S., & Zilles, K. (2009). Receptor architecture of human cingulate cortex: Evaluation of the four-region neurobiological model. *Human Brain Mapping*, 30, 2336–2355.

Pannunzi, M., Hindriks, R., Bettinardi, R. G., Wenger, E., Lisofsky, N., Martensson, J., ... Deco, G. (2017). Resting-state fMRI correlations: From link-wise unreliability to whole brain stability. *NeuroImage*, 157, 250–262.

Passow, S., Specht, K., Adamsen, T. C., Biermann, M., Brekke, N., Craven, A. R., ... Hugdahl, K. (2015). Default-mode network functional connectivity is closely related to metabolic activity. *Human Brain Mapping*, 36, 2027–2038.

Pijnenburg, R., Scholtens, L. H., Mantini, D., Vanduffel, W., Barrett, L. F., & van den Heuvel, M. P. (2019). Biological characteristics of connection-wise resting-state functional connectivity strength. *Cerebral Cortex*, 29, 4646–4653.

Pizzagalli, D. A. (2011). Frontocingulate dysfunction in depression: Toward biomarkers of treatment response. *Neuropsychopharmacology*, 36, 183–206.

Power, J. D., Barnes, K. A., Snyder, A. Z., Schlaggar, B. L., & Petersen, S. E. (2012). Spurious but systematic correlations in functional connectivity MRI networks arise from subject motion. *NeuroImage*, 59, 2142–2154.

Provencher, S. W. (2001). Automatic quantitation of localized in vivo 1H spectra with LCModel. *NMR in Biomedicine*, 14, 260–264.

Puts, N. A. J., Edden, R. A. E., Evans, C. J., McGlone, F., & McGonigle, D. J. (2011). Regionally specific human GABA concentration correlates with tactile discrimination thresholds. *The Journal of Neuroscience*, 31, 16556–16560.

Robertson, C. E., Ratai, E.-M., & Kanwisher, N. (2016). Reduced GABAergic action in the autistic brain. *Current Biology*, 26, 80–85.

Satterthwaite, T. D., Elliott, M. A., Gerraty, R. T., Ruparel, K., Loughead, J., Calkins, M. E., ... Wolf, D. H. (2013). An improved framework for confound regression and filtering for control of motion artifact in the preprocessing of resting-state functional connectivity data. *NeuroImage*, 64, 240–256.

Schaefer, A., Kong, R., Gordon, E. M., Laumann, T. O., Zuo, X.-N., Holmes, A. J., ... Yeo, B. T. T. (2018). Local-global Parcellation of the human cerebral cortex from intrinsic functional connectivity MRI. *Cerebral Cortex*, 28, 3095–3114.

Shannon, B. J., Dosenbach, R. A., Su, Y., Vlassenko, A. G., Larson-Prior, L. J., Nolan, T. S., ... Raichle, M. E. (2012). Morning-evening variation in human brain metabolism and memory circuits. *Journal of Neurophysiology*, 109, 1444–1456.

Shehzad, Z., Kelly, A. M. C., Reiss, P. T., Gee, D. G., Gotimer, K., Uddin, L. Q., ... Milham, M. P. (2009). The resting brain: Unconstrained yet reliable. *Cerebral Cortex*, 19, 2209–2229.

Shipp, S. (2007). Structure and function of the cerebral cortex. *Current Biology*, 17, R443–R449.

Smith S.M., Miller K.L., Salimi-Khorshidi G., Webster M., Beckmann C.F., Nichols T.E., ... Woolrich M.W. (2011). Network modelling methods for FMRI. *NeuroImage*, 54, (2), 875–891. http://dx.doi.org/10.1016/j.neuroimage.2010.08.063

Spielberg, J. M., Miller, G. A., Heller, W., & Banich, M. T. (2015). Flexible brain network reconfiguration supporting inhibitory control. *PNAS*, 112, 10020–10025.

Stagg, C. J., Bachtiar, V., Amadi, U., Gudberg, C. A., Ilie, A. S., Sampaio-Baptista, C., ... Johansen-Berg, H. (2014). Local GABA concentration is related to network-level resting functional connectivity. *eLife*, 3, e01465.

Stagg, C. J., Best, J. G., Stephenson, M. C., O'Shea, J., Wylezinska, M., Kincses, Z. T., ... Johansen-Berg, H. (2009). Polarity-sensitive modulation of cortical neurotransmitters by transcranial stimulation. *The Journal of Neuroscience*, 29, 5202–5206.

Stevens, F. L., Hurley, R. A., & Taber, K. H. (2011). Anterior cingulate cortex: Unique role in cognition and emotion. *The Journal of Neuropsychiatry and Clinical Neurosciences*, 23(2), 121–125. https://doi.org/10.1176/jnp.23.2.jnp121

Stevenson, I. H., Rebesco, J. M., Miller, L. E., & Körding, K. P. (2008). Inferring functional connections between neurons. *Current Opinion in Neurobiology*, 18, 582–588.

Suárez, L. E., Markello, R. D., Betzel, R. F., & Misic, B. (2020). Linking structure and function in macroscale brain networks. *Trends in Cognitive Sciences*, 24, 302–315.

Tagliazucchi, E., Balenzuela, P., Fraiman, D., Montoya, P., & Chialvo, D. R. (2011). Spontaneous BOLD event triggered averages for estimating functional connectivity at resting state. *Neuroscience Letters*, 488, 158–163.

Tak, S., Polimeni, J. R., Wang, D. J. J., Yan, L., & Chen, J. J. (2015). Associations of resting-state fMRI functional connectivity with flow-BOLD coupling and regional vasculature. *Brain Connectivity*, 5, 137–146.

Takado, Y., Takuwa, H., Sampei, K., Urushihata, T., Takahashi, M., Shimojo, M., ... Higuchi, M. (2021). MRS-measured glutamate versus GABA reflects excitatory versus inhibitory neural activities in awake mice. *The Journal of Cerebral Blood Flow & Metabolism*, 42, 197–212.

Takagi, Y., Hirayama, J., & Tanaka, S. C. (2019). State-unspecific patterns of whole-brain functional connectivity from resting and multiple task states predict stable individual traits. *NeuroImage*, 201, 116036.

Thayer, J. F., Åhs, F., Fredrikson, M., Sollers, J. J., III, & Wager, T. D. (2012). A meta-analysis of heart rate variability and neuroimaging studies: Implications for heart rate variability as a marker of stress and health. *Neuroscience & Biobehavioral Reviews*, 36, 747–756.

Vallat, R. (2018). Pingouin: Statistics in python. *Journal of Open Source Software*, 3, 1026.

van den Heuvel, M. P., Scholtens, L. H., Turk, E., Mantini, D., Vanduffel, W., & Feldman Barrett, L. (2016). Multimodal analysis of cortical chemoarchitecture and macroscale fMRI resting-state functional connectivity. *Human Brain Mapping*, 37, 3103–3113.

van Heukelum, S., Mars, R. B., Guthrie, M., Buitelaar, J. K., Beckmann, C. F., Tiesinga, P. H. E., ... Havenith, M. N. (2020). Where is cingulate cortex? A cross-species view. *Trends in Neurosciences*, 43, 285–299.

Wang, K., Smolker, H. R., Brown, M. S., Snyder, H. R., Hankin, B. L., & Banich, M. T. (2020). Association of γ-aminobutyric acid and glutamate/glutamine in the lateral prefrontal cortex with patterns of intrinsic functional connectivity in adults. *Brain Structure & Function*, 225, 1903–1919.

Wang, Z., Chen, L. M., Négyessy, L., Friedman, R. M., Mishra, A., Gore, J. C., & Roe, A. W. (2013). The relationship of anatomical and

functional connectivity to resting-state connectivity in primate somatosensory cortex. *Neuron, 78*, 1116–1126.

Wilson, G. H., Yang, P.-F., Gore, J. C., & Chen, L. M. (2016). Correlated inter-regional variations in low frequency local field potentials and resting state BOLD signals within S1 cortex of monkeys: Correlation between LFP and resting state fMRI signals. *Human Brain Mapping, 37*, 2755–2766.

Yu, C., Zhou, Y., Liu, Y., Jiang, T., Dong, H., Zhang, Y., & Walter, M. (2011). Functional segregation of the human cingulate cortex is confirmed by functional connectivity based neuroanatomical parcellation. *Neuroimage, 54*, 2571–2581.

Zhou, Y., Friston, K. J., Zeidman, P., Chen, J., Li, S., & Razi, A. (2018). The hierarchical oganization of the default, dorsal attention and salience networks in adolescents and young adults. *Cerebral Cortex, 28*, 726–737.

SUPPORTING INFORMATION

Additional supporting information may be found in the online version of the article at the publisher's website.